ChemPubSoc Europe

DOI: 10.1002/cssc.201301037

Sol–Gel Synthesis of Aliovalent Vanadium-Doped $LiNi_{0.5}Mn_{1.5}O_4$ Cathodes with Excellent Performance at High Temperatures

Min Chul Kim,[a] Kyung-Wan Nam,*[b] Enyuan Hu,[b] Xiao-Qing Yang,[b] Hyungsub Kim,[c] Kisuk Kang,[c] Vanchiappan Aravindan,[a, d] Woo-Seong Kim,[e] and Yun-Sung Lee*[a]

Extraordinary performance at elevated temperature is achieved for high-voltage spinel-phase $LiNi_{0.5}Mn_{1.5}O_4$ cathodes prepared using an adipic-acid-assisted sol–gel technique and doped with vanadium. V-substitution in the Li sites (Wykoff position 8a) is confirmed by V K-edge X-ray absorption spectroscopy and Rietveld refinement ($Li_{0.995}V_{0.005}Ni_{0.5}Mn_{1.5}O_4$). V-doped $LiNi_{0.5}Mn_{1.5}O_4$ delivered a reversible capacity of approximately 130 and 142 mAh g^{-1} at ambient and elevated temperature conditions, respectively. Furthermore, the $Li_{0.995}V_{0.005}Ni_{0.5}Mn_{1.5}O_4$ phase rendered approximately 94% and 84% of initial capacity compared to approximately 85% and 3% for the $LiNi_{0.5}Mn_{1.5}O_4$ phase after 100 cycles in ambient and elevated temperature conditions, respectively. The enhancements are mainly because of the suppression of Mn dissolution and unwanted side reaction with electrolyte counterpart, and to the increase in conductivity, improving the electrochemical profiles for the V-doped phase.

Introduction

In the recent past, research in the area of high-voltage cathodes for Li-ion batteries (LIBs) has been directed towards development of high energy density Li-ion power packs to drive hybrid electric vehicles (HEV) and electric vehicles (EV).[1–6] The construction of LIB with such high energy density depends on the utilization of high-voltage cathode materials, as graphitic anodes essentially serve as a host matrix during the charge–discharge process.[7–10] Among these high-voltage cathode materials, Ni-substituted spinel ($LiNi_{0.5}Mn_{1.5}O_4$) is appealing due to its high operating potential (≈4.7 V vs. Li), cost-effectiveness, ease of preparation, and eco-friendliness compared to other conventional cathodes such as $LiCoO_2$ (≈4 V vs. Li), $LiMn_2O_4$ (≈4 V vs. Li), and $LiFePO_4$ (≈3.4 V vs. Li).[7,10–13] However, the higher redox potential of transition metals in $LiNi_{0.5}Mn_{1.5}O_4$ cathodes exceeds the thermodynamic stability of conventional carbonate-based electrolyte solutions (≈4.6 V vs. Li), resulting in poor electrochemical performance at both ambient and elevated temperature conditions.[14] Conversely, zero-emission transportation applications such as HEV and EV require LIB with a long life span and good performance at elevated temperature.[4] Generally, at elevated temperature conditions, the electrolytes are prone to accelerated side reactions, which results in the formation of an inactive mass over the active material and, subsequently, delivers poor electrochemical performance.[11,14] Therefore, achieving a spinel-phase cathode with good performance at elevated temperature condition is quite challenging. It is well known that spinel $LiNi_{0.5}Mn_{1.5}O_4$ cathodes exist in two polymorphs, either in a well-ordered (containing only Mn^{4+}) or a disordered (comprising Mn^{3+} and Mn^{4+}) structure. The ordered structure provides very flat charge/discharge profiles at approximately 4.7 V vs. Li, whereas discrete curves result for the case of a disordered structure.[3,13,15] This clearly illustrates that the synthesis technique plays a vital role in yielding high-performance spinel-phase cathodes with a well-ordered structure and high energy density. Regarding co-doping, several isovalent materials, including Ti, Ru, Cr, Al, Zr, and Ru, have been used to substitute either the Ni or Mn site; F-doping has also been carried out for oxygen sites to improve cycleability.[16] Surface modifications with metals (Au, Ag, and Zn), metal oxides (ZrO_2, SnO_2, and ZnO), phosphates (ZrP_2O_7 and Li_3PO_4), and fluorides (BiOF) have also been carried out to improve cycleability, especially at high temperature operations. Further additional time-consuming treatment is required to apply such coatings and a small reduction of Mn^{4+} to Mn^{3+} is inevitable during such coating process.[13,15] Moreover, these

[a] M. C. Kim, Dr. V. Aravindan, Prof. Y.-S. Lee
Faculty of Applied Chemical Engineering
Chonnam National University
Gwang-ju 500-757 (Korea)
E-mail: leeys@chonnam.ac.kr

[b] Dr. K.-W. Nam, E. Hu, Dr. X.-Q. Yang
Chemistry Department
Brookhaven National Laboratory
Upton, NY 11973 (USA)
E-mail: knam@bnl.gov

[c] H. Kim, Prof. K. Kang
Department of Materials Science and Engineering
Seoul National University
Seoul 151-742 (Korea)

[d] Dr. V. Aravindan
Energy Research Institute @ NTU (ERI@N)
Nanyang Technological University
637553 (Singapore)

[e] Dr. W.-S. Kim
GS EM co. Ltd
Iksan 570-977 (Korea)

cathodes do not exhibit performances adequate for use in high energy density LIB. However, to date, no work has been reported on the metal-doping on Li (8a) sites of spinel-phase $LiNi_{0.5}Mn_{1.5}O_4$, though such Li-site doping certainly provides improvement in the electrochemical performance of the cathodes.[17] The main advantage of introducing such an aliovalent element is the dramatic improvement in the electrochemical characteristics. Herle et al.[17] and Chung et al.[18] convincingly showed this for the olivine-phase $LiFePO_4$ cathode by doping small amounts of various aliovalent elements such as Mg^{2+}, Al^{3+}, Ti^{4+}, Zr^{4+}, Nb^{5+}, or W^{6+} in Li-sites; they observed an eight orders of magnitude enhancement in conductivity. In this study, we substitute, for the first time, aliovalent vanadium (V^{5+}) in the Li sites of a spinel-phase compound ($LiNi_{0.5}Mn_{1.5}O_4$) by using a scalable sol–gel technique mediated by adipic acid. Though an extensive examination of the existing physical and electrochemical studies has been previously performed and is described here in detail, to the best of our knowledge, no work has been reported on aliovalent V-doping in an Ni-substituted spinel ($Li_{0.995}V_{0.005}Ni_{0.5}Mn_{1.5}O_4$).

Results and Discussion

Figure 1a represents the XRD patterns of parent ($LiNi_{0.5}Mn_{1.5}O_4$) and V-substituted ($Li_{0.995}V_{0.005}Ni_{0.5}Mn_{1.5}O_4$) spinel-phase compounds. In Figure 1a, no significant differences between the reflections are observed and sharp reflections clearly indicate the formation of a highly crystalline spinel structure with the $Fd\bar{3}m$ space group. Lattice parameter values are calculated by Rietveld refinement and found to be $a = 8.158(8)$ Å and 8.158(7) Å for $LiNi_{0.5}Mn_{1.5}O_4$ and $Li_{0.995}V_{0.005}Ni_{0.5}Mn_{1.5}O_4$, respectively. The observed values are consistent with the previous reports in the literature and no significant difference is observed between the parent and V-doped phases.[11,13] This may be due to the use of a significantly smaller amount of dopant with a smaller ionic radius (V^{5+}, 68 pm) than Li. Therefore, we assume the occupancy of V in Li (8a) sites of spinel-phase $Li_{0.995}V_{0.005}Ni_{0.5}Mn_{1.5}O_4$ cathodes. However, a trace amount of unavoidable $Li_xNi_{1-x}O$ (PDF No. 01-077-2023) impurity was observed for both $LiNi_{0.5}Mn_{1.5}O_4$ and $Li_{0.995}V_{0.005}Ni_{0.5}Mn_{1.5}O_4$ phases (Figure S1). The XRD pattern of as-prepared $LiNi_{0.5}Mn_{1.5}O_4$ sample shows the additional super-structure peaks indicating Ni–Mn cation ordering in the structure. This cation ordering in the *16d* octahedral sites of the $Fd\bar{3}m$ spinel structure transforms the *16d* Wyckoff positions to two *4b* and *12d* positions of the $P4_332$ spinel structure.[19] The XRD pattern of $Li_{0.995}V_{0.005}Ni_{0.5}Mn_{1.5}O_4$ shows a slight decrease in Ni–Mn ordering peaks in spite of a small amount of V doping. Further, a decrease in the intensity of the impurity phases is also noted after the incorporation of V. Therefore, we believe that the vanadium doping in the $P4_332$ structure causes the disordering of cations on the transition-metal sub-lattice though the V atoms prefer to occupy the Li sites. Generally, this cation ordering in the spinel structure is known to deteriorate the electrochemical properties of the spinel lattice.[19] In order to prove the occupancy of transition metal in Li sites, V K-edge X-ray absorption near edge structure (XANES) spectra were recorded

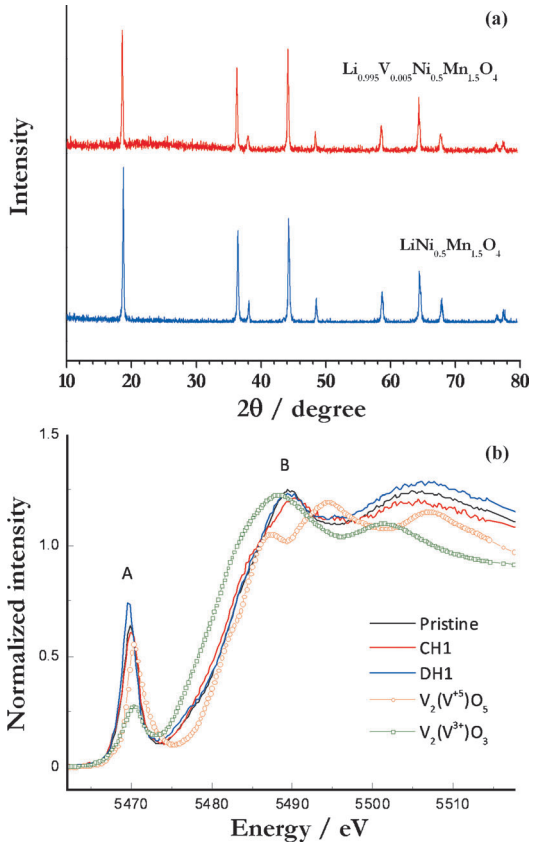

Figure 1. (a) XRD patterns of bare and V-doped spinel-phase $LiNi_{0.5}Mn_{1.5}O_4$, (b) Vanadium K edge XANES spectra of $Li_{0.995}V_{0.005}Ni_{0.5}Mn_{1.5}O_4$ cathode along with first charge (CH1) and discharged conditions (DH1). The XANES spectra of V_2O_5 and V_2O_3 are also given for reference.

and are illustrated in Figure 1b. The K edge XANES spectra of the reference compounds (e.g., $V_2(V)O_5$ and $V_2(III)O_3$) were also measured and compared. In all spectra, two distinct edge features are observed and are marked as A and B. The pre-edge peak is associated with the dipole-forbidden 1s→3d electronic transition, which is partially allowed through the quadrupole electronic transition in which the 3d and 4p orbitals hybridize because of the lack of an inversion center of symmetry, or because of structural distortion in local symmetry between the transition metals and oxygen coordination. Therefore, transition-metal XANES spectra usually show much stronger pre-edge peak intensity in the tetrahedral sites than in the octahedral sites, due to the lack of an inversion center in the tetrahedral coordination symmetry. The strong main absorption peak B originates from the electronic-dipole-allowed transition of a 1s core electron to an unoccupied 4p orbital. A comparison of the edge position of the V-doped sample with the reference compounds, as shown in Figure 1b, reveals that the average oxidation state of V is close to 5+. Indeed, the very strong pre-edge peak intensity observed for the sample suggests the tetrahedral occupancy of V. Furthermore, it is well known that V^{5+} is energetically more stable in tetrahedral sites than in octahedral sites due to its electronic configuration (i.e., empty d shells, d^0 configuration) and small ionic size (i.e., effective ionic radius 0.355 Å).[20,21] However, many reports suggest the pres-

ence of V^{5+} in tetrahedral sites stabilized in the spinel-structured oxides, which are synthesized by various synthetic methods other than the adipic-acid-assisted sol–gel technique.[22–24] Therefore, this strongly suggests that the V substitution in the Li sites is due to the thermodynamically originated process rather than the synthesis technique adopted in the present work. During the 1st cycle, the local structure and average valance state of V remain unchanged, suggesting that V is not involved in the redox reaction. However, the slight increase of intensity in the pre-edge peak A after the 1st discharge reveals a possible light local structural distortion around V after the cycle.

Surface morphological features of the obtained Ni-doped and V-co-doped spinel-phase compounds were analyzed through SEM and TEM and are illustrated in Figures 2 a–f. The SEM and TEM images clearly show the particulate morphology, which is irregular in shape for both cases (Figure 2 c–f). A slight increase in size of the spinel particles is observed in the case of the V-doped $LiNi_{0.5}Mn_{1.5}O_4$ phase. From the TEM images, it can be seen that the particle sizes are between 100 and 200 nm with some aggregation. The HR-TEM images reveal the highly crystalline nature of the Ni-doped and V-co-doped spinel-phase compounds.

Electrochemical Li-insertion properties were evaluated in a half-cell assembly between 3.5 and 5 V vs. Li at a current density of 0.8 mA cm^{-2} in both ambient and elevated temperature (55 °C) conditions. Typical galvanostatic charge–discharge curves of spinel-phase materials recorded in ambient temperature are illustrated in Figure 3 a. Both spinel-phase materials displayed very flat operating potential at approximately 4.7 V vs. Li and delivered a discharge capacity of approximately 138 mAh g^{-1}, which corresponds to the reversible insertion of approximately 0.95 moles of Li. The appearance of a long distinct plateau indicates the presence of Mn^{4+} ions in the matrix and corresponds to a well-ordered structure.[10,11] The observed flat plateaus in the charge–discharge process originate from the $Ni^{2+/4+}$ redox couple, as the $Mn^{4+/5+}$ couple is electrochemically inactive.[13] It is interesting to note that the presence of V in the spinel matrix leads to a marginal increase in the polarization of the electrode. On the other hand, the $Li_{0.995}V_{0.005}Ni_{0.5}Mn_{1.5}O_4$ delivers excellent electrochemical properties compared to the native phase (Figure 3 b). As expected, both the spinel-phase compounds experience capacity

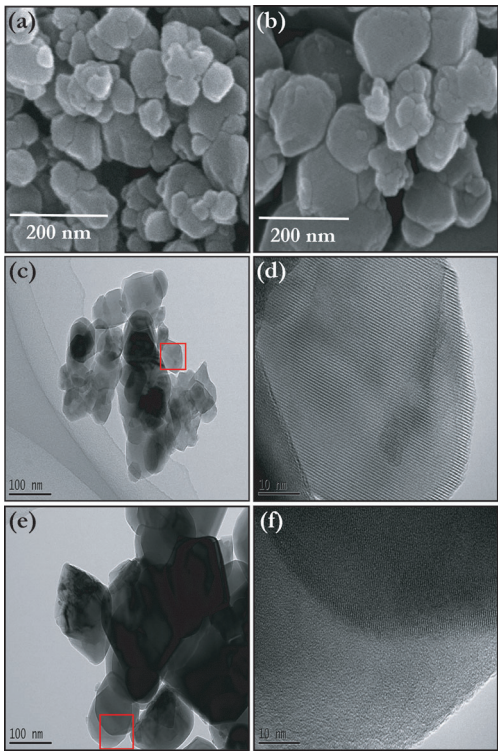

Figure 2. (a) SEM image of $LiNi_{0.5}Mn_{1.5}O_4$ material. (b) SEM image of $Li_{0.995}V_{0.005}Ni_{0.5}Mn_{1.5}O_4$ material. (c–d) TEM images of $LiNi_{0.5}Mn_{1.5}O_4$ material, (e–f) TEM images of $Li_{0.995}V_{0.005}Ni_{0.5}Mn_{1.5}O_4$ material.

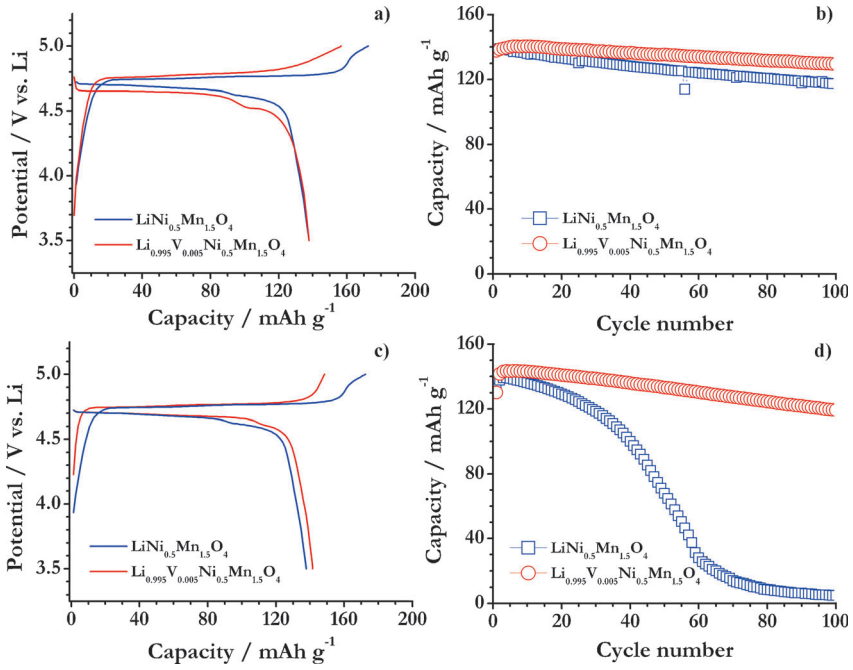

Figure 3. (a) Typical galvanostatic charge–discharge curves (second cycle) of spinel-phase $LiNi_{0.5}Mn_{1.5}O_4$ and $Li_{0.995}V_{0.005}Ni_{0.5}Mn_{1.5}O_4$ powders in half-cell configuration at ambient temperature conditions with a current density of 0.8 mA cm^{-2}. (b) Plot of discharge capacity vs. cycle number. (c) Typical galvanostatic charge–discharge traces of spinel-phase $LiNi_{0.5}Mn_{1.5}O_4$ and $Li_{0.995}V_{0.005}Ni_{0.5}Mn_{1.5}O_4$ powders in half-cell configuration at elevated temperature conditions (55 °C) with current density of 0.8 mA cm^{-2}. (b) Plot of discharge capacity vs. cycle number in elevated temperature conditions (55 °C)

fade during cycling, which is normal because of the reactivity of cathode active particles with the electrolyte solution [as the operating potential of the $Ni^{2+/4+}$ redox couple (≈4.7 V vs. Li) exceeds the thermodynamic stability (≈4.6 V vs. Li) window of carbonate based solutions[2,5]]. In addition, Mn dissolution cannot be ruled out for such fading.[5] In ambient conditions, reversible capacity of approximately 117 and 130 mAh g^{-1} is observed after 100 galvanostatic cycles for the $LiNi_{0.5}Mn_{1.5}O_4$ and $Li_{0.995}V_{0.005}Ni_{0.5}Mn_{1.5}O_4$ powders, respectively. Irrespective of doping, both spinel-phase materials undergo electrolyte decomposition, which results in higher charge capacity than theoretical limitations. Moreover, such a higher charge capacity is common for such Ni-doped spinel-phase compounds. V-doped $LiNi_{0.5}Mn_{1.5}O_4$ retains approximately 94% of initial discharge capacity, which is approximately 9% higher than the native-phase material (≈85%). Note that the half-cell comprising $Li_{0.995}V_{0.005}Ni_{0.5}Mn_{1.5}O_4$ powders exhibits slightly higher polarization than that comprising the native-phase material. Good performance at elevated temperature is critical for the development of high energy density Li-ion power packs.[1,4,9,12] Hence, galvanostatic cycling studies were carried out at a current density of 0.8 mA cm^{-2} in elevated temperature conditions and are presented in Figures 3c–d. The test cell delivered discharge capacities of approximately 138 and 142 mAh g^{-1} for $LiNi_{0.5}Mn_{1.5}O_4$ and $Li_{0.995}V_{0.005}Ni_{0.5}Mn_{1.5}O_4$, respectively. In contrast to ambient temperature, a significantly smaller polarization was observed for $Li_{0.995}V_{0.005}Ni_{0.5}Mn_{1.5}O_4$ than for the parent phase, which is mainly due to the improvement in the electronic conductivity profiles of said phase. Nazar et al.[17] noted a similar enhancement in electrical profiles for aliovalent substituted (Zr^{4+}) Li sites in the olivine-phase $LiFePO_4$. Chung et al.[18] also confirmed such increase in conductivity profiles (eight orders of magnitude) by incorporating aliovalent substitution in the Li sites of the olivine-phase ($Li_{1-x}M_xFePO_4$, where $M = Mg^{2+}$, Al^{3+}, Ti^{4+}, Zr^{4+}, Nb^{5+}, or W^{6+}). At elevated conditions, the reactions are highly accelerated; therefore, a high reactivity resulted for the parent $LiNi_{0.5}Mn_{1.5}O_4$ cathode compared to $Li_{0.995}V_{0.005}Ni_{0.5}Mn_{1.5}O_4$. As a result, a drastic fade in the capacity profiles is noted compared to the $Li_{0.995}V_{0.005}Ni_{0.5}Mn_{1.5}O_4$ powders. After 100 cycles, the test cells showed a capacity of approximately 3% and 84% for $LiNi_{0.5}Mn_{1.5}O_4$ and $Li_{0.995}V_{0.005}Ni_{0.5}Mn_{1.5}O_4$, respectively. The remarkable improvement in the capacity retention properties is mainly attributed to the V doping in Li sites, which might prevent transition-metal dissolution and subsequently reduce the severe reactivity of the cathode towards electrolyte solutions, and particularly towards HF attack.[17] The transition-metal dissolution in bare $LiNi_{0.5}Mn_{1.5}O_4$ (Mn: 20.1 ppm and Ni: 7.44 ppm) compared to the $Li_{0.995}V_{0.005}Ni_{0.5}Mn_{1.5}O_4$ phase (Mn: 5.51 ppm and Ni: 4.4 ppm) was evidenced by ICP analysis after cycling at elevated conditions. We are certain that the cation disordering caused from vanadium doping enhances the charge-transfer (CT) reaction and cycle performances. Additionally, we speculate that the surface segregation of vanadium dopants stabilizes the thick solid–electrolyte interphase (SEI) layer, and this layer significantly enhances the cycle performances by suppressing the transition-metal dissolution.[19] On the other hand, a thick SEI layer results in the slight increase in polarization of the electrode at ambient temperature compared to native compound (Figure 3a). In order to study the dissolution properties of Mn at ambient conditions, both powders were stored in electrolyte solution for one week in ambient conditions and subjected to ICP analysis. As expected, Mn dissolution was found to be severe for the parent compound (41.9 ppm) compared to the V-doped phase (18.6 ppm). After one week storage under electrolyte solutions, the active materials were harvested and tested in a half-cell configuration to measure the influence of V doping on the electrochemical properties at elevated temperature conditions at a current density of 0.8 mA cm^{-2}, as illustrated in Figure 4. From the galvanostatic profiles, for an initial discharge capacity of approximately 102 mAh g^{-1} and 112 mAh g^{-1}, for $LiNi_{0.5}Mn_{1.5}O_4$ and $Li_{0.995}V_{0.005}Ni_{0.5}Mn_{1.5}O_4$, respectively, a considerable amount of capacity drop can be observed (≈26% drop for $LiNi_{0.5}Mn_{1.5}O_4$ and ≈21% drop for $Li_{0.995}V_{0.005}Ni_{0.5}Mn_{1.5}O_4$). After 60 cycles, a similarly abrupt capacity drop occurs in the electrochemical profiles of $LiNi_{0.5}Mn_{1.5}O_4$ compounds before and after storage in the electrolyte solutions. On the other hand, extraordinary cycling profiles are noted for the case of $Li_{0.995}V_{0.005}Ni_{0.5}Mn_{1.5}O_4$ cathodes after storage and approximately 86% of the initial reversible capacity is retained. The observed capacity is consistent with the electrochemical performance before storage. This result clearly indicates the dramatic improvement in the electrochemical performance of the high-voltage cathode Li-

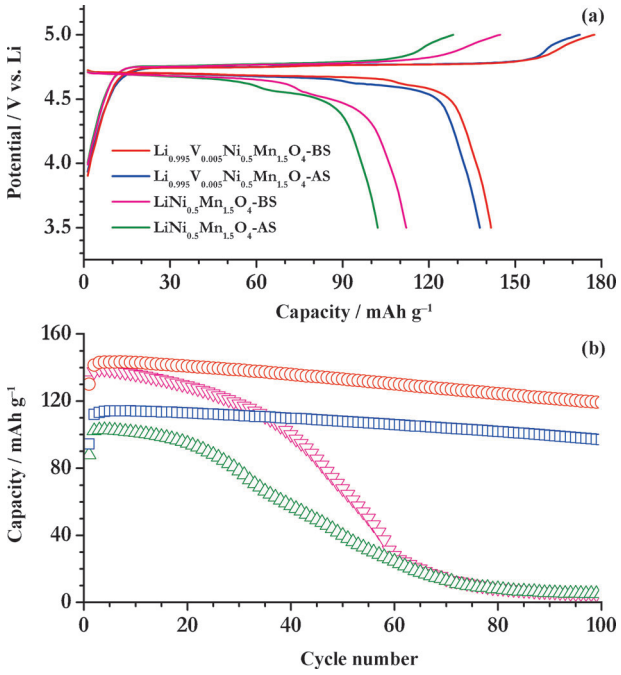

Figure 4. (a) Typical galvanostatic charge–discharge traces (second cycle) of spinel-phase $LiNi_{0.5}Mn_{1.5}O_4$ and $Li_{0.995}V_{0.005}Ni_{0.5}Mn_{1.5}O_4$ powders in half-cell configuration at elevated temperature conditions (55 °C) with a current density of 0.8 mA cm^{-2} after storage in electrolyte solution for one week. (b) Plot of discharge capacity vs. cycle number in elevated temperature conditions (55 °C). ($Li_{0.995}V_{0.005}Ni_{0.5}Mn_{1.5}O_4$-BS: ○, $Li_{0.995}V_{0.005}Ni_{0.5}Mn_{1.5}O_4$-AS: □, $LiNi_{0.5}Mn_{1.5}O_4$-BS: ▽, $LiNi_{0.5}Mn_{1.5}O_4$-AS: △, BS: before storage, AS: after storage).

$Ni_{0.5}Mn_{1.5}O_4$ brought about by the addition of V in Li-sites, irrespective of ambient and elevated conditions. This result certainly provides a platform for the development of such high-voltage cathodes by a simple sol–gel process.

In order to validate the reactivity of spinel-phase cathodes with electrolyte solutions in both ambient and elevated temperature conditions, electrochemical impedance spectroscopy (EIS) measurements were carried out and presented in Figure 5. The Nyquist plot can be separated into three main segments as follows: first, the presence of a high-frequency

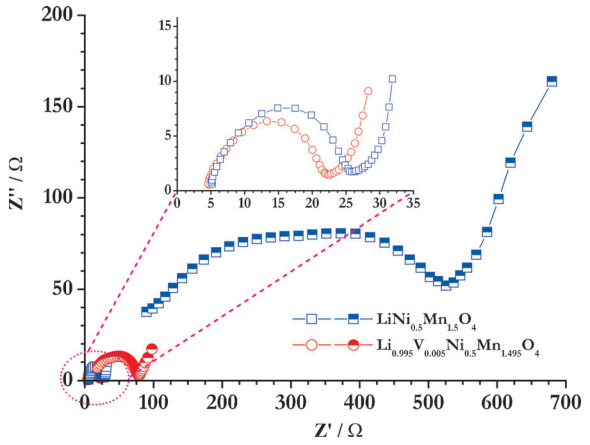

Figure 5. Electrochemical impedance measurements of $LiNi_{0.5}Mn_{1.5}O_4$ and $Li_{0.995}V_{0.005}Ni_{0.5}Mn_{1.5}O_4$ cathodes recorded in two-electrode coin-cell configurations before and after cycling at elevated temperature conditions. Inset: EIS traces before cycling.

semicircle is attributed to the formation of a solid electrolyte interface film and/or contact resistance; secondly, the medium frequency region is ascribed to the CT impedance across the electrode/electrolyte interface; and, finally, the vertical tail inclined approximately 45° towards the real axis corresponds to the Li-diffusion kinetics and the so-called Warburg tail.[25] As expected, aliovalent V-doping in the spinel-phase material improves the conduction profiles, which is clearly evident from the inset in Figure 5. The resistance of approximately 5 Ω for both cells is attributed to the impedance offered by the electrolyte solution used. On the other hand, a dramatic increase in CT resistance is noted after cycling at 55 °C for $LiNi_{0.5}Mn_{1.5}O_4$ (from ≈26 to ≈525 Ω) compared to the $Li_{0.995}V_{0.005}Ni_{0.5}Mn_{1.5}O_4$ phase (from ≈22 to ≈78 Ω). This clearly indicates the vigorous reactivity of the electrode towards the electrolyte solution (originating from severe HF attack), which leads to the faster decomposition of electrolyte and subsequently forms an unwanted mass over the active material surface.[26,27] This unwanted by-product on the surface hinders the Li-ion diffusion properties during cycling, resulting in an increase in CT resistance.[26,27] Concurrently, a drastic increase in solution resistance is observed (≈80 and ≈19 Ω for $LiNi_{0.5}Mn_{1.5}O_4$ and $Li_{0.995}V_{0.005}Ni_{0.5}Mn_{1.5}O_4$ powders, respectively) because of the dissolution of Mn atoms in the electrolyte solution, which increases the viscosity of the medium and subsequently inhibits the mobility of Li-ions.[5,28] As a result, poor electrochemical profiles are noted for the parent-phase compound. This study clearly demonstrates a substantial enhancement in the electrochemical performance of spinel-phase $LiNi_{0.5}Mn_{1.5}O_4$ cathodes at elevated temperature conditions and in high-voltage electrolytes through a small amount of V doping in Li-sites. This scalable, one-step synthesis procedure does not involve surface modifications and provides a platform for the development of high energy density Li-ion power packs and possible applications for zero emission transportation.

Conclusions

A high performance V-doped $LiNi_{0.5}Mn_{1.5}O_4$ cathode was successfully prepared using an sol–gel process mediated by adipic acid. An exceptional electrochemical profile was observed at elevated temperature and approximately 84% of initial reversible capacity was retained compared to the parent-phase compound (≈3%) after 100 cycles. The enhancement was mainly because of the V doping in Li-sites, which prevents Mn dissolution, and suppresses the reactivity between electrode and electrolyte. This result could facilitate the development of high-voltage cathodes (high energy density Li-ion batteries) without any surface modifications in a single step scalable process.

Experimental Section

A sol–gel method was used to synthesize the spinel-phase $LiNi_{0.5}Mn_{1.5}O_4$ powders with and without V doping as described in our previous work.[15] In a typical procedure, all analytical grade starting materials such as $Li(CH_3COO)\cdot H_2O$ (Junsei Chem, Japan), $Ni(CH_3COO)\cdot 4H_2O$ (Aldrich, USA), and $Mn(CH_3COO)\cdot 4H_2O$ (Aldrich, USA) were dissolved separately according to the stoichiometric ratio in distilled water. They were then mixed with the appropriate amount of chelating agent, adipic acid ($C_6H_{10}O_4$, Sigma–Aldrich, USA), and stirred continuously at 90 °C to yield a precursor powder. The precursor powder was precalcined at approximately 450 °C for 10 h to decompose the acetate moieties. The intermediate product was collected, pelletized, and heat treated at 700 °C for 12 h to obtain single-phase $LiNi_{0.5}Mn_{1.5}O_4$ powders. The same procedure was repeated for the V-doped spinel phase by using V_2O_5 (Sigma–Aldrich, USA) as the source.

A powder X-ray diffractometer (Rint 1000, Rigaku, Japan) equipped with a Cu K_α radiation source was used to study the structural properties. The surface morphology of the powder was analyzed by field emission scanning electron microscopy (FE-SEM, S4700, Hitachi, Japan) and transmission electron microscopy (TEM, TECNAI, Philips, The Netherlands). The X-ray adsorption spectroscopy (XAS) data were measured at the X19 A beamline of National Synchrotron Light Source (NSLS) at Brookhaven National Laboratory (BNL) using the Si(111) double-crystal monochromator. The V K-edge spectra were collected in a fluorescence mode using a 4-element silicon drift detector (Vortex, ME4) (due to very low concentration of V), whereas the Mn and Ni K-edge spectra were measured in a conventional transmission mode. The reference metallic foils were placed after the samples and measured simultaneously with the sample spectra for energy calibration. The XAS data were processed using the Athena programs.[29] A CR2032 coin-cell assembly was used for the electrochemical characterization. The composite test electrodes were fabricated with 20 mg of accurately weighed active material, 3 mg conductive additive (super P), and 3 mg of

teflonized acetelene black (TAB-2). The resulting film was pressed over a 200 mm^2 stainless steel mesh current collector. The half-cells were assembled with a composite cathode and a metallic lithium anode separated by porous polypropylene film (Celgard 3401, USA) filled with 1 M $LiPF_6$ in ethylene carbonate/dimethyl carbonate (1:1 by vol., Soulbrain Co., Ltd., Korea) solution. Electrochemical impedance measurement was carried out in a half-cell assembly ($Li/LiNi_{0.5}Mn_{1.5}O_4$ or $Li_{0.995}V_{0.005}Ni_{0.5}Mn_{1.5}O_4$) using a Bio-Logic electrochemical work station (SP-150, Biologic, France), in which metallic lithium served as both a working and a counter electrode. Galvanostatic cycling studies were carried out between 3.5 and 5 V vs. Li under ambient and elevated temperature (55 °C) conditions at a constant current density of 0.8 mA cm^{-2}.

Acknowledgements

This study was supported by the IT R&D program of MKE/KEIT (KI10039182, "Development of 5 V cathode material which capacity is 125 mAh g^{-1} & high-voltage electrolyte which decomposition is over 5 V for lithium secondary battery"). The work at BNL was supported by the U.S. Department of Energy, the Assistant Secretary for Energy Efficiency and Renewable Energy, Office of Vehicle Technologies under Contract Number DE-AC02-98CH10886.

Keywords: batteries · electrochemistry · high-voltage cathode · lithium · sol–gel

[1] V. Aravindan, J. Gnanaraj, Y.-S. Lee, S. Madhavi, *J. Mater. Chem. A* **2013**, *1*, 3518 – 3539.
[2] J. B. Goodenough, K.-S. Park, *J. Am. Chem. Soc.* **2013**, *135*, 1167 – 1176.
[3] J. B. Goodenough, Y. Kim, *Chem. Mater.* **2010**, *22*, 587 – 603.
[4] E. J. Cairns, P. Albertus, *Annu. Rev. Chem. Biomol. Eng.* **2010**, *1*, 299 – 320.
[5] O. K. Park, Y. Cho, S. Lee, H.-C. Yoo, H.-K. Song, J. Cho, *Energy Environ. Sci.* **2011**, *4*, 1621 – 1633.
[6] S. Y. Hong, Y. Kim, Y. Park, A. Choi, N.-S. Choi, K. T. Lee, *Energy Environ. Sci.* **2013**, *6*, 2067 – 2081.
[7] A. Kraytsberg, Y. Ein-Eli, *Adv. Energy Mater.* **2012**, *2*, 922 – 939.
[8] M. Hu, X. Pang, Z. Zhou, *J. Power Sources* **2013**, *237*, 229 – 242.
[9] C. M. Julien, A. Mauger, *Ionics* **2013**, *19*, 951 – 988.
[10] M. Kim, S. Kim, V. Aravindan, W. Kim, S. Lee, Y. Lee, *J. Electrochem. Soc.* **2013**, *160*, A1003 – A1008.
[11] R. Santhanam, B. Rambabu, *J. Power Sources* **2010**, *195*, 5442 – 5451.
[12] M. M. Thackeray, C. Wolverton, E. D. Isaacs, *Energy Environ. Sci.* **2012**, *5*, 7854 – 7863.
[13] J. Song, D. W. Shin, Y. Lu, C. D. Amos, A. Manthiram, J. B. Goodenough, *Chem. Mater.* **2012**, *24*, 3101 – 3109.
[14] V. Aravindan, J. Gnanaraj, S. Madhavi, H.-K. Liu, *Chem. Eur. J.* **2011**, *17*, 14326 – 14346.
[15] Y. S. Lee, Y. K. Sun, S. Ota, T. Miyashita, M. Yoshio, *Electrochem. Commun.* **2002**, *4*, 989 – 994.
[16] Q. Liu, S. Wang, H. Tan, Z. Yang, J. Zeng, *Energies* **2013**, *6*, 1718 – 1730.
[17] P. S. Herle, B. Ellis, N. Coombs, L. Nazar, *Nat. Mater.* **2004**, *3*, 147 – 152.
[18] S.-Y. Chung, J. T. Bloking, Y.-M. Chiang, *Nat. Mater.* **2002**, *1*, 123 – 128.
[19] D. W. Shin, C. A. Bridges, A. Huq, M. P. Paranthaman, A. Manthiram, *Chem. Mater.* **2012**, *24*, 3720 – 3731.
[20] J. B. Goodenough, A. L. Loeb, *Phys. Rev.* **1955**, *98*, 391 – 408.
[21] X. Ma, G. Hautier, A. Jain, R. Doe, G. Ceder, *J. Electrochem. Soc.* **2013**, *160*, A279 – A284.
[22] O. N. Leonidova, V. I. Voronin, I. A. Leonidov, R. F. Samigullina, B. V. Slobodin, *J. Struct. Chem.* **2003**, *44*, 243 – 247.
[23] G. T. K. Fey, W. Li, J. R. Dahn, *J. Electrochem. Soc.* **1994**, *141*, 2279 – 2282.
[24] D. Prakash, Y. Masuda, C. Sanjeeviraja, *Ionics* **2013**, *19*, 17 – 23.
[25] V. Aravindan, K. Karthikeyan, K. S. Kang, W. S. Yoon, W. S. Kim, Y. S. Lee, *J. Mater. Chem.* **2011**, *21*, 2470 – 2475.
[26] J. S. Gnanaraj, E. Zinigrad, L. Asraf, M. Sprecher, H. E. Gottlieb, W. Geissler, M. Schmidt, D. Aurbach, *Electrochem. Commun.* **2003**, *5*, 946 – 951.
[27] J. S. Gnanaraj, M. D. Levi, Y. Gofer, D. Aurbach, M. Schmidt, *J. Electrochem. Soc.* **2003**, *150*, A445 – A454.
[28] J. Cho, T.-J. Kim, Y. J. Kim, B. Park, *Chem. Commun.* **2001**, 1074 – 1075.
[29] B. Ravel, M. Newville, *J. Synchrotron Radiat.* **2005**, *12*, 537 – 541.

Received: September 28, 2013
Revised: November 12, 2013
Published online on January 7, 2014